Proceedings of 2017 IEEE
International Conference on Mechatronics and Automation
August 6 - 9, Takamatsu, Japan

Installation Angle Offset Compensation of Puncture Robot Based on Measurement of Needle by CT Equipment

Akisato Nagao, Takayuki Matsuno,
Kazusi Kimura, Tetsushi Kamegawa, Mamoru Minami
Graduate School of Natural Science and Technology
Okayama University
1-1-1 Tsushimanaka, Kita-ku, Okayama city, Okayama 700-8530, Japan
pxn81vhp@s.okayama-u.ac.jp

Takao Hiraki
Department of Radiology
Okayama University Hospital
2-5-1 Shikata, Kita-ku, Okayama city, Okayama 700-8558, Japan
takaoh@tc4.so-net.ne.jp

***Abstract*— A medical procedure called Interventional Radiology(IR) is paid much attention in recent years. IR can be performed percutaneously while a doctor observes patient' s fluoroscopic image. Therefore this surgical method is low-invasiveness method. In this surgery, computed tomography (CT) equipment is often used. But a doctor is exposed to strong radiation from CT. Thus, we have developed a remote-controlled surgery support robot called "Zerobot". Because Zerobot is placed front of CT equipment by human, an angle offset from installation target position occurs. If a doctor punctures without noticing that Zerobot has an installation angle offset, there is danger of hurting the part that should not be hurt around a target cancer. In order to solve this problem, we propose an angle offset compensation method and the installation angle offset derivation method using a CT equipment is proposed. Then, effectiveness of proposed method is confirmed through experiments.**

***Index Terms*— Surgery Support Robot, Interventional Radiology, Puncture Robot**

I. Introduction

There is a surgical method called Interventional Radiology (IR). This surgical method is conducted with imaging modality such as CT and X-rays. With observing medical images, the surgeon conducts IR treatment percutaneously with inserting a needle or a catheter to the patient body. In particular, CT equipment has high visibility and objectivity. And CT fluoroscopy system, which can show medical images in real time, is superior as guiding tool for IR. So CT-guided IR is applied to lung cancer treatment, liver cancer treatment, biopsy, and so on [1]. The appearance of manual IR treatment is shown in **Fig. 1**. As compared with conventional survey, IR can be conducted in local anesthesia and this surgical method is minimally-invasive to patients. Moreover patients can be discharged from the hospital about three or four days after treatment. Because of these advantages, IR is paid much attention in recent years. According to the opinion of a doctor, the minimum size of cancer is 5 [mm]. Therefore an operator must puncture a needle carefully and accurately. In addition, operators are exposed to radiation during CT fluoroscopy because operators conduct procedure close to the CT gantry.

Fig. 1. Interventional Radiology

In order to prevent radiation exposure, operators wear radiation protection aprons and handle a needle using a forceps which is useful to make distance between hand and CT measure plane. However, it is impossible to prevent radiation exposure completely. Then some medical robots are developed in order to improve accuracy of positioning of a needle, and to reduce radiation exposure, such as AcuBot[2], CT-Bot[3] and MAXIO[4]. These robots aim to support operators to insert a needle as CT-guided puncture. However, Zerobot, which is developed by our research group, aims to conduct whole process from positioning robot to inserting a needle by remote-control.

In this research, in order to seek the problem of Robotic IR system, we have conducted phantom puncture experiment[5] and animal puncture experiment[6]. In previous research, we implemented the automatic targeting function. Firstly, a doctor specifies the current needle tip position and the canner position with the CT equipment. Secondly, a computer calculates amounts of movement of each axis to make the needle tip pose before puncturing. The doctor operates the Zerobot by NC operation based on this calculation result. This function reduces CT scan time and reduces patient exposure. However, this function does not consider an installation angle offset of Zerobot. Therefore, if Zerobot is

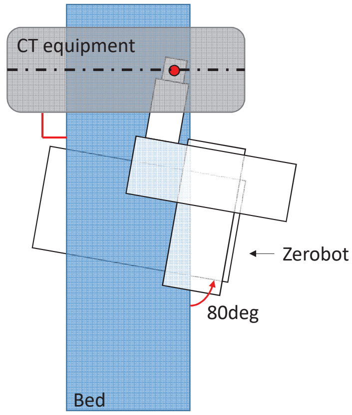

Fig. 2. Zerobot setting position

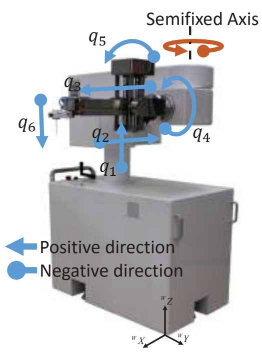

Fig. 3. Appearance of Zerobot

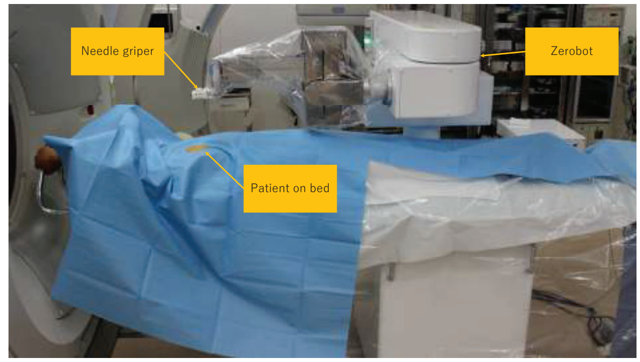

Fig. 4. Reproduction of surgical environment

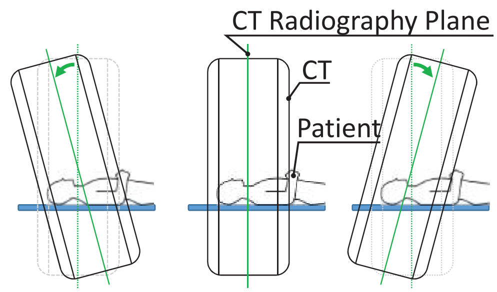

Fig. 5. Definition of CT Radiography Plane

not installed parallel to the CT equipment, it is impossible to bring the needle tip to the target pose correctly. Since Zerobot is installed onto of floor surgical room by human, an angle offset around vertical axis from installation target position occurs (**Fig. 2**). If a doctor punctures without noticing that Zerobot has the installation angle offset, there is danger of hurting organs that most not be hurt around a target cancer. Therefore, we propose a method to compensate installation angle offset between Zerobot and CT equipment.

II. Mechanism

The appearance of Zerobot is shown in **Fig. 3**. It has five DOF for needle tip position and needle direction, and has one DOF for puncturing direction. Six actuators are in the machine. Four linear actuators (X, Y, Z and puncturing axes directions) and two rotational actuators (around the X and Y axes) are included.

Therefore, Zerobot can perform puncture operation by actuating the puncturing axis, regardless of the posture. Four passive wheels are mounted on the bottom of the robot, so it can be moved with human power. At the surgical operation, the robot is located under a bed and fixed by locking the wheels (**Fig. 4**). Changing needle direction and puncturing are performed in CT-gantry by arm part above patient.

Because of a method to reconstruct image by CT equipments, if a metal part was in the gantry, incorrect image called artifact will appear on CT image. If artifact appearers, patient's internal image will be obscured and trouble will occur on an surgical operation. Therefore, metal parts cannot be used on needle gripper. Accordingly parts are made of engineering plastic, which is radiolucent material. Motor for puncture is required in end-effector. The angle of elevation of CT equipment can be changed as necessary, as shown in **Fig. 5**.

III. Kinematics Analysis

Zerobot has six active joints and a semifixed joint as shown in **Fig. 3**. Each axis' positive direction is represented by arrows. Semifixed axis is fixed to -90[deg] or 90[deg] as shown in **Fig. 6**. Six active axes' angle[deg] or displacement[mm] is defined as $\boldsymbol{q} = [q_1, q_2, \ldots, q_6]^T$. q_1, q_2, q_3 and q_6 are linear axes, and q_4 and q_5 are rotation axes. And needle tip position and needle posture are defined as ${}^0\boldsymbol{r}_E = [x, y, z, \phi_A, \phi_B]^T$. ϕ_A and ϕ_B are defined as **Fig. 6**. ϕ_A is the angle of needle on the CT radiography plane, and ϕ_B is the gantry tilt angle of the plane. Since the needle is line symmetric, five variables ignoring the rotation around the center axis of the needle are output. Forward kinematics is projection of vector from $\boldsymbol{q}$ to ${}^0\mathbf{r_E}$, and inverse kinematics is projection of vector from ${}^0\boldsymbol{r}_E$ to $\boldsymbol{q}$. Hereafter, $\sin\theta$ is represented as S_θ, and $\cos\theta$ is represented as C_θ. Moreover, there is one thing that should be noted here. Originally, in the all of equations for kinematics elements of C_{α_3} should be included (Definition of α_3 is

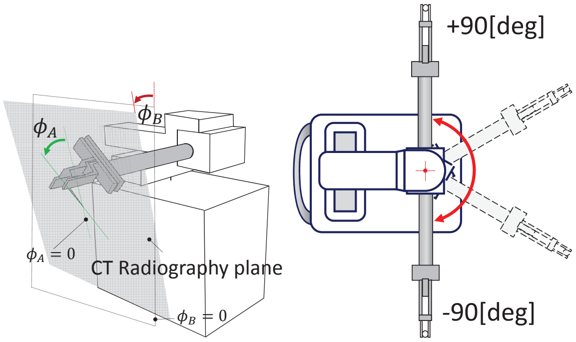

Fig. 6. Important parameters in the kinematics. Left side is definition of ϕ_A and ϕ_B, and right side is states image which can be taken by semifixed axis.

TABLE I
DH PARAMETERS

i	α_{i-1}	a_{i-1}	d_i	θ_i
1	0	0	q_1	0
2	-90	0	q_2	-90
3	90	0	$q_3 - l_3$	0
4	90 or -90	0	l_1	$180 + q_4$
5	-90	l_2	0	$90 + q_5$
6	90	0	q_6	0

described in after this subsection.). But α_3 can only take the value of 90[deg] or -90[deg]. In this case, the value of C_{α_3} must be zero. Therefore, elements of C_{α_3} are omitted from all of equations for kinematics in this paper.

A. Forward Kinematics

Forward kinematics of Zerobot is derived by Denavit-Hartenberg notaion (DH notaion)[7]. Location of coordinate systems is listed in **Fig. 7**. These coordinate systems are located following DH notaion. DH parameters are shown in **Table I**. In the table, the value of α_3 depends on semifixed axis direction. And definition of required parameters l_1, l_2 and l_3 is also shown in **Fig. 7**. So we can calculate ${}^0\boldsymbol{T}_6$, which is homogeneous transformation matrix from Σ_0 to Σ_6. And ${}^6\boldsymbol{T}_E$ is just translate transformation depending on needle length defined as l_E. Therefore, ${}^0\boldsymbol{T}_E$ can be calculated as follows.

$$
{}^0\boldsymbol{T}_E = \begin{bmatrix} -S_{q_4}S_{q_5}S_{\alpha_3} & C_{q_4}S_{\alpha_3} & S_{q_4}C_{q_5}S_{\alpha_3} & {}^0r_{Ex} \\ C_{q_5}S_{\alpha_3} & 0 & S_{q_5}S_{\alpha_3} & {}^0r_{Ey} \\ C_{q_4}S_{q_5} & S_{q_4} & -C_{q_4}C_{q_5} & {}^0r_{Ez} \\ 0 & 0 & 0 & 1 \end{bmatrix}, \quad (1)
$$

$$
\begin{aligned}
{}^0r_{Ex} &= l_3 - q_3 + l_2 S_{q_4} S_{\alpha_3} + (q_6 + l_9 + l_E) S_{q_4} C_{q_5} S_{\alpha_3} + l_7 S_{q_4} S_{q_5} S_{\alpha_3}, \\
{}^0r_{Ey} &= (q_6 + l_9 + l_E) S_{q_5} S_{\alpha_3} + q_2 - l_1 S_{\alpha_3} + l_7 C_{q_5} S_{\alpha_3}, \\
{}^0r_{Ez} &= q_1 - l_2 C_{q_4} - (q_6 + l_9 + l_E) C_{q_4} C_{q_5} - l_7 C_{q_4} C_{q_5}.
\end{aligned}
$$

Next, ϕ_A and ϕ_B corresponded to needle posture should be calculated. Then, direction vector of needle represented on Σ_0 is defined as ${}^0\boldsymbol{n}_E$. ${}^0\boldsymbol{n}_E$ equals third column direction vector

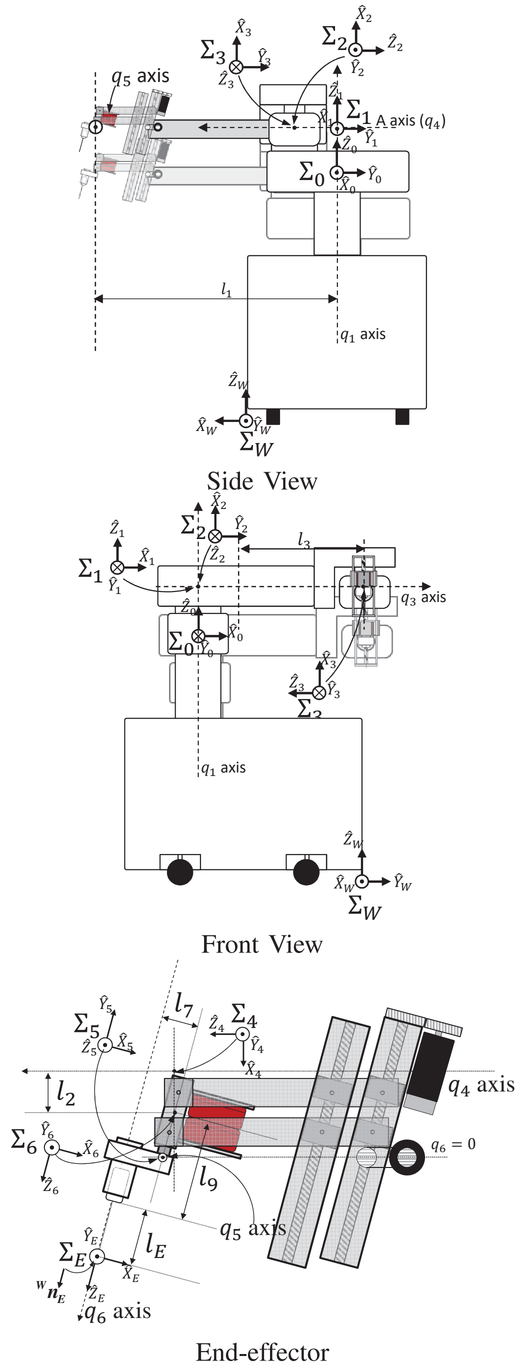

Fig. 7. Location of Coordinate Systems

of rotation matrix of ${}^{0}\boldsymbol{T}_E$. Therefore ${}^{0}\boldsymbol{n}_E$ is represented as (2).

$$
{}^{0}\boldsymbol{n}_E = \left[\begin{array}{ccc} S_{q_4}C_{q_5}S_{\alpha_3} & S_{q_5}S_{\alpha_3} & -C_{q_4}C_{q_5} \end{array}\right]^T_. \tag{2}
$$

Here, ${}^{0}\boldsymbol{n}_E$ also can be represented with ϕ_A and ϕ_B as follow. When we make the rotation matrix including ϕ_A and ϕ_B which can coincide direction of z axis of Σ_0 with $\hat{Z}_E$ direction, third column direction vector of the rotation matrix is ${}^{0}\boldsymbol{n}_E$.

$$
\begin{aligned}
{}^{0}\boldsymbol{n}_E &= \boldsymbol{R}_{\boldsymbol{x}(-\pi/2)}\boldsymbol{R}_{\boldsymbol{z}(\alpha_3)}\boldsymbol{R}_{\boldsymbol{x}(\phi_B)}\boldsymbol{R}_{\boldsymbol{y}(\phi_A)}\begin{bmatrix} 0 \\ 0 \\ 1 \end{bmatrix} \\
&= \begin{bmatrix} S_{\alpha_3}S_{\phi_A} \\ S_{\alpha_3}C_{\phi_A}S_{\phi_B} \\ -C_{\phi_A}C_{\phi_B} \end{bmatrix}_.
\end{aligned} \tag{3}
$$

As comparing between (2) and (3), ϕ_A and ϕ_B can be calculated as (4), (5).

$$
\phi_B = \tan^{-1}\left(\frac{1}{C_{q_4}}\tan q_5\right), \tag{4}
$$

$$
\phi_A = \tan^{-1}\left(C_{\phi_B}\tan q_4\right). \tag{5}
$$

Finally, ${}^{0}\boldsymbol{r}_E$ is calculated as (6).

$$
{}^{0}\boldsymbol{r}_E = \begin{bmatrix} l_3 - q_3 + l_2 S_{q_4}S_{\alpha_3} + q_6 S_{q_4}C_{q_5}S_{\alpha_3} + l_E S_{q_4}C_{q_5}S_{\alpha_3} \\ q_6 S_{q_5}S_{\alpha_3} + q_2 - l_1 S_{\alpha_3} + l_E S_{q_5}S_{\alpha_3} \\ q_1 - l_2 C_{q_4} - q_6 C_{q_4}C_{q_5} - l_E C_{q_4}C_{q_5} \\ \tan^{-1}\left(C_{\phi_B}\tan q_4\right) \\ \tan^{-1}\left(\frac{1}{C_{q_4}}\tan q_5\right) \end{bmatrix}_. \tag{6}
$$

B. Inverse Kinematics

In this subsection, procedure of inverse kinematics is described. Target needle tip position is defined as ${}^{0}\boldsymbol{r}^*_E = [x^*, y^*, z^*, \phi^*_A, \phi^*_B]^T$. And target robot posture is defined as $\boldsymbol{q}^* = [q^*_1, q^*_2, \ldots, q^*_6]^T$. According to (6), relationship between $\boldsymbol{q}^*$ and ${}^{0}\boldsymbol{r}^*_E$ is represented as follows.

$$
x^* = (l_E + q_6)\, S_{q^*_4}C_{q^*_5}S_{\alpha_3} + l_2 S_{q^*_4}S_{\alpha_3} + l_3 - q^*_3, \tag{7}
$$

$$
y^* = (l_E + q_6)\, S_{q^*_5}S_{\alpha_3} - l_1 S_{\alpha_3} + q^*_2, \tag{8}
$$

$$
z^* = q^*_1 - l_2 C_{q^*_4} - (l_E + q_6)\, C_{q^*_4}C_{q^*_5}, \tag{9}
$$

$$
\phi^*_B = \tan^{-1}\left(\frac{1}{C_{q^*_4}}\tan q^*_5\right), \tag{10}
$$

$$
\phi^*_A = \tan^{-1}\left(C_{\phi^*_B}\tan q^*_4\right). \tag{11}
$$

Inverse kinematics can be derived from (7) to (11). But Zerobot has redundant DOF. Therefore we derived inverse kinematics in under the assumption that q_6, which is puncture axis, is fixed and is known. Then, inverse kinematics is

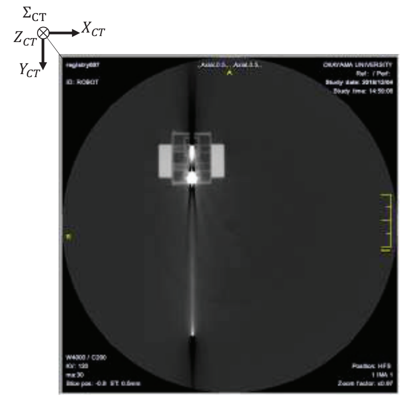

Fig. 8. CT coordinate system

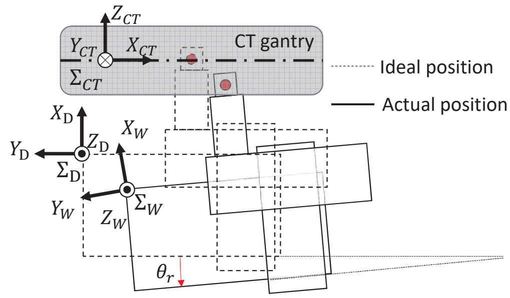

Fig. 9. Doctor coordinate system

derived as follows.

$$
q^*_4 = \tan^{-1}\left(\frac{1}{C_{\phi^*_A}}\tan\phi^*_B\right), \tag{12}
$$

$$
q^*_5 = \tan^{-1}\left(C_{q^*_4}\tan\phi^*_A\right), \tag{13}
$$

$$
q^*_1 = z^* + l_2 C_{q^*_4} + (l_E + q_6)\, C_{q^*_4}C_{q^*_5}, \tag{14}
$$

$$
q^*_2 = l_1 S_{\alpha_3} - (l_E + q_6)\, S_{q^*_5}S_{\alpha_3} + y^*, \tag{15}
$$

$$
q^*_3 = l_2 S_{q^*_4}S_{\alpha_3} + (l_E + q_6)\, S_{q^*_4}C_{q^*_5}S_{\alpha_3} + l_3 - x^* \tag{16}
$$

IV. Installation Angle Offset Compensation Method

A. Coordinate Systems

Since CT images are used for our experiment, a coordinate system of the CT image should be defined as **Fig. 8**. The pixel size of CT in this paper is fixed as 0.8 [mm/pixel] A coordinate system of the doctor's point of view is also defined as **Fig. 9** X_{CT} and Y_D have opposite direction each other, on the other hands, Z_{CT} and X_D have same direction.

B. Method of Estimate the installation Angle offset of Zerobot

In order to compensate installation angle offset of Zerobot, it is necessary to estimate the installation angle offset. After installing Zerobot to the position as shown in **Fig. 4**, first the z_{CT} position of the needle with CT equipment is measured. Secondly, Zerobot is operated to move along with y_W

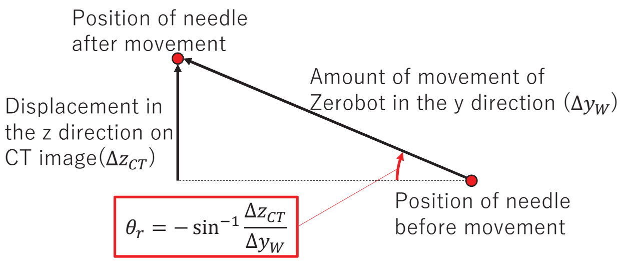

Fig. 10. Derivation of angle offset

direction by 20 mm and the z_{CT} position of the needle is measured. This procedure is repeated until the y_W becomes 200 mm. A first order approximation equation is obtained using the least squares method.

$$z_{CT} = a\, y_W + b \tag{17}$$

The relationship between a center position of needle tip center and a angle offset of Zerobot can be obtained a following equation according to **Fig. 10**.

$$\theta_r = -\sin^{-1}\left(\frac{\Delta z_{CT}}{\Delta y_W}\right). \tag{18}$$

Experiments to measure the robot installation angle offset is described later.

C. Calculation of Target Value

In this subsection, the method to compensate a motion of robot based on amount of Zerobot installation angle offset is described. A needle tip target pose $\left[{}^D x_E^*, {}^D y_E^*, {}^D z_E^*, {}^D \phi_A^*, {}^D \phi_B^*\right]$ in coordinate system Σ_D is converted into target pose in coordinate system Σ_W. The doctor viewpoint coordinate system (Σ_D) is converted to the coordinate system of the robot viewpoint (Σ_W) by the following rotation matrics.

$$\begin{aligned} {}^W\boldsymbol{T}_D &= \begin{bmatrix} \cos\theta_r & -\sin\theta_r & 0 \\ \sin\theta_r & \cos\theta_r & 0 \\ 0 & 0 & 1 \end{bmatrix}^{-1} \\ &= \begin{bmatrix} \cos\theta_r & \sin\theta_r & 0 \\ -\sin\theta_r & \cos\theta_r & 0 \\ 0 & 0 & 1 \end{bmatrix}. \end{aligned} \tag{19}$$

Firstly, a needle tip target position is converted by a following equation.

$$\begin{aligned} \begin{bmatrix} x_E^* \\ y_E^* \\ z_E^* \end{bmatrix} &= {}^W\boldsymbol{T}_D \begin{bmatrix} {}^D x_E^* \\ {}^D y_E^* \\ {}^D z_E^* \end{bmatrix} \\ &= \begin{bmatrix} {}^D x_E^* \cos\theta_r + {}^D y_E^* \sin\theta_r \\ -{}^D x_E^* \sin\theta_r + {}^D y_E^* \cos\theta_r \\ {}^D z_E^* \end{bmatrix}. \end{aligned} \tag{20}$$

Secondly, needle tip target posture is converted by the following equation.

$$\begin{aligned} \boldsymbol{n}_E^* &= {}^W\boldsymbol{T}_D {}^D\boldsymbol{n}_E^* \\ &= \begin{bmatrix} S_{\alpha_3} S_{{}^D\phi_A^*} \cos\theta_r + S_{\alpha_3} C_{{}^D\phi_A^*} S_{{}^D\phi_B^*} \sin\theta_r \\ -S_{\alpha_3} S_{{}^D\phi_A^*} \sin\theta_r + S_{\alpha_3} C_{{}^D\phi_A^*} S_{{}^D\phi_B^*} \cos\theta_r \\ -C_{{}^D\phi_A^*} C_{{}^D\phi_B^*} \end{bmatrix}. \end{aligned} \tag{21}$$

ϕ_A^* and ϕ_B^* are calculated using first and second rows of (21).

$$\phi_A^* = \sin^{-1}\left(S_{{}^D\phi_A^*} \cos\theta_r + C_{{}^D\phi_A^*} S_{{}^D\phi_B^*} \sin\theta_r\right), \tag{22}$$

$$\phi_B^* = \sin^{-1}\left(\frac{-S_{{}^D\phi_A^*} \sin\theta_r + C_{{}^D\phi_A^*} S_{{}^D\phi_B^*} \cos\theta_r}{C_{\phi_A^*}}\right). \tag{23}$$

Values obtained by (20), (22) and (23) are substituted into the eqs from (12) to (16). This method realizes functions that a doctor can control Zerobot along with cordinate system Σ_D even thought installation angle θ_r exists.

V. Experiment

A. Estimate the installation Angle offset of Zerobot

In order to compensate an installation angle offset, first the offset is measured by using CT equipment. Experiment procedure to measure the installation angle offset was written in subsection IV. B. Zerobot is installed with approximately -10 [deg] against CT equipment by setting the Zerobot at about 80 [deg] against a side of the bed (**Fig. 2**). The result of the experiment is described below. First of all, the installation angle offset of Zerobot is calculated from the amount of movement of Zerobot y_W-axis and the amount of movement of CT coordinate system in the z_{CT} direction. To measure the position of the needle, images of the needle are extracted from the image group at each operating position. In order to decide needle tip position on z_{CT} direction, a feasible image should be selected. In this paper, an image which has the brightest needle is selected. However, when the extracted images are an even number, select the image owing a longer needle pare is selected as shown in (**Fig.11**). When the Y_W axis is 0 [mm], the deviation from each operating position with Z_{CT} as the origin is taken as the movement amount of the needle in the Z_{CT} direction.

An approximate straight line equation can be calcurated as $z_{CT} = 0.175\, y_W$ from **Fig. 12** . The installation angle offset of Zerobot is -10.08 [deg] from (18) and the approximate straight line equation. It is almost equal to the installation angle of Zerobot and it can be said that the measurement is successful.

B. Installation Angle Offset Compensation

After estimation of installation angle offset θ_r, desired hand position of robot is calculated according to equations from (21) to (24). First, θ_r = -10.08 [deg] is set in those equations in order to calculate compensated desired position in this experiment. Next hand position of robot moves in

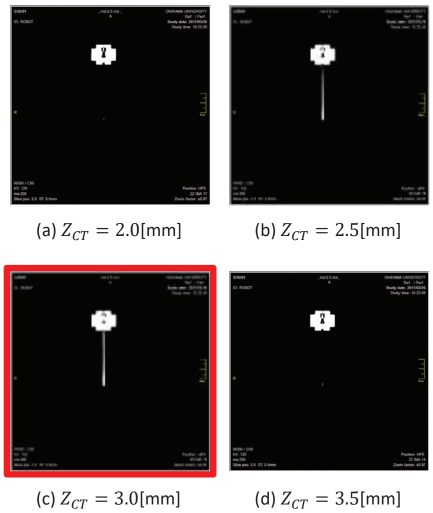

Fig. 11. Needle center position of Z_{CT} direction. In that case, the needle center position is (c).

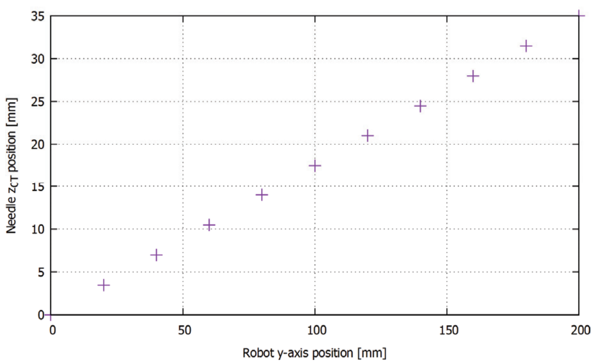

Fig. 12. Amount of movement in the z_{CT} direction during Zerobot y-axis operation

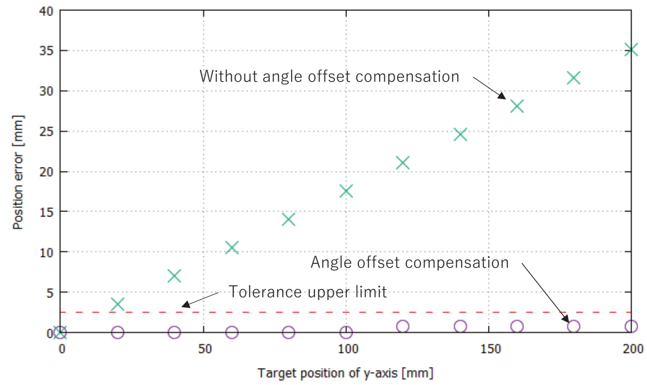

Fig. 13. Needle tip center position error when moving Zerobot in Y_D direction with an installation angle offset of -10.08 degree

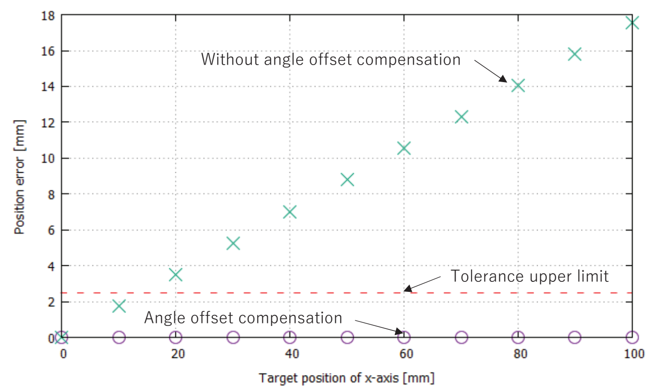

Fig. 14. Needle tip center position error when moving Zerobot in X_D direction with an installation angle offset of -10.08 degree

Y_D direction from 0 [mm] to 200 [mm] per 20 [mm]. In each pose, CT scanning is conducted to acquire the position of needle tip so as to obtain deviation in Y_D direction. Amount of X_D-axis and Y_D-axis direction motions of doctor coordinate system are verified from the taken image. The experiment result is shown in **Fig. 13**. We define an error tolerance in Y_D position to 2.5 [mm] because the minimum diameter of the cancer is 5 [mm]. In the operation without compensation, the center position of the needle greatly deviates from the tolerance error. However, keeping the maximum value of error within tolerance is succeed by angle offset compensation control.

Secondly, the motion accuracy is verified in X_D-axis direction. The position of needle is measured each time while the robot moves along X_D direction from 0 [mm] to 100 [mm] per 10 [mm]. **Fig. 14** shows the error when the robot moves in the X_D direction. When operating the robot in the x-axis direction with the angle offset compensation function, the needle tip center position error cannot be founded. **Fig. 13** and **14** show that the angle offset compensation controls in the orthogonal direction were successful.

Next, the rotation motion accuracy around ϕ_A-axis direction is verified. As shown in the **Fig. 15** , the angle error is measured with the inner product of the unit vector of the ideal needle posture $\left[{}^{I}x_{CT}, {}^{I}y_{CT}, {}^{I}z_{CT}\right]$ and the unit vector of the actual needle posture $\left[{}^{A}x_{CT}, {}^{A}y_{CT}, {}^{A}z_{CT}\right]$ as (24). Unit vector of the actual needle posture is measured from the deviation of the tip and the root position of the needle based on the CT image.

$$\theta_{error} = \cos^{-1}\left({}^{A}x_{CT}{}^{I}x_{CT} + {}^{A}y_{CT}{}^{I}y_{CT} + {}^{A}z_{CT}{}^{I}z_{CT}\right) \quad (24)$$

Tolerance of the angle is set to 1.43 [deg] or less. Because the needle tip deviation should be suppressed within 2.5 [mm] when puncturing 100 [mm].

$$\sin^{-1}\left(\frac{2.5}{100}\right) = 1.43\,[\text{deg}] \quad (25)$$

The posture of needle is measured each time while the robot rotates around ϕ_A direction from -80 [deg] to 80 [deg] per 10 [deg]. **Fig. 16** shows amount of angle error. In the operation

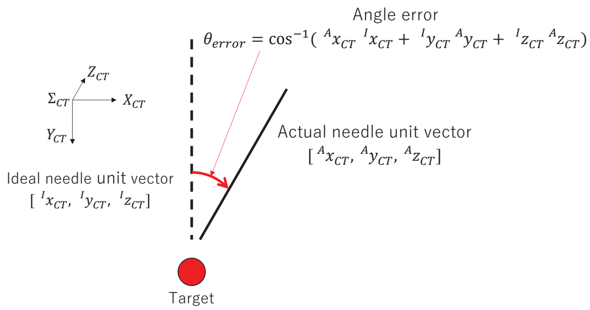

Fig. 15. Measurement method of angle error

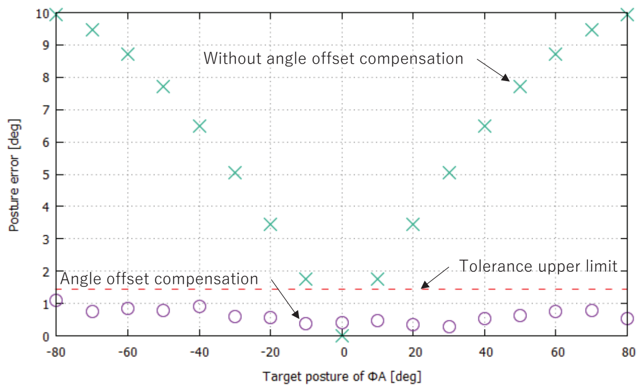

Fig. 16. Needle posture error when rotating hand of Zerobot around ϕA direction with an installation angle offset of -10.08 degree

without compensation, the posture of needle also greatly deviates from the tolerance error. Same as position, posture error can also be adjusted to the allowable error by angle offset compensation.

Finally, the motion accuracy in ϕ_B-axis direction is verified. The posture of needle is measured each time while the robot rotates around ϕ_B direction from -10 [deg] to 10 [deg] per 2 [deg]. **Fig. 17** shows amount of angle error. A decreasing phenomena of error due to installation angle error compensation is confirmed as in the other results. It can be seen that the error after angle offset compensation is within the allowable range.

Fig. 16 and **17** show that the posture compensation is also successful. However, it can be seen **Fig. 17** that the error without compensation is so small that compensation is not necessary in this case, so that no significant effect of compensation is seen.

VI. Conclusion

We have developed Zerobot, a interventional radiology support robot, to eliminate doctor exposure. Zerobot can be automatically operated to a target pose. However, the installation angle offset of the robot was not considered when using this function. Therefore, a method to compensation of installation angle offset using CT equipment is proposed. The

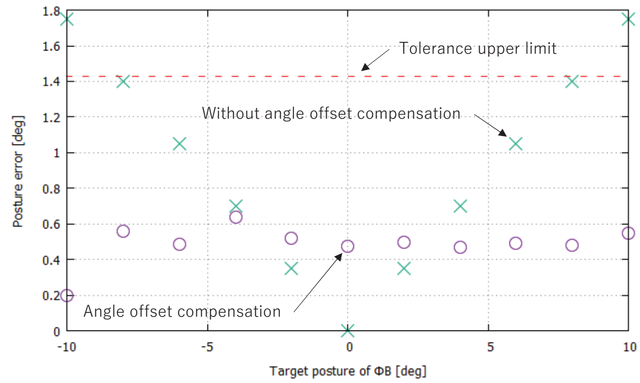

Fig. 17. Needle posture error when rotating hand of Zerobot around ϕB direction with an installation angle offset of -10.08 degree

installation angle offset compensation is successful on all axis. Finally motion compensation will be implemented in automatic targeting and remote center.

Acknowledgment

This work was supported by MEXT KAKENHI Grant Number 17K10439 and Research on Development of New Medical Devices 15652923 from Japan Agency for Medical Research and Development, AMED.

References

[1] Takao Hiraki, Tetsushi Kamegawa, Takayuki Matsuno, Susumu Kanazawa, "Development of a Robot for CT Fluoroscopy-guided Intervention : Free Physicians from Radiation", Jon J Intervent Radiol, 20:375-381, 2014.

[2] Dan Staianovici, Kevin Cleary, Alexandru Patriciu, Dumitru Mazilu, Alexandru Stanimir, Nicolae Craciunoiu, Vance Watson, Louis Kavoussi, "AcuBot: A Robot for Radiological Interventions", IEEE TRANSACTIONS ON ROBOTICS AND AUTOMATION, VOL.19, NO.5, pp.927-930, OCTOBER 2003.

[3] Benjamin Maurin, Bernard Bayle, Olivier Piccin, Jacques Gangloff, Michel de Mathelin, Christophe Doignon, Philippe Zanne, Afshin Gangi, "A Patient-Mounted Robotic Platform for CT-Scan Guided Procedures", IEEE TRANSACTIONS ON BIOMEDICAL ENGINEERING, VOL.55, NO.10, OCTOBER, 2008.

[4] Yilun Koethe, Sheng Xu, Gnanasekar Velusamy, Bradford J. Wood, Aradhana M. Venkatesan, "Accuracy and efficacy of percutaneous biopsy and ablation using robotic assistance under computed tomography guidance: a phantom study", European Radiology, Volume 24, Issue 3, pp 723-730, March 2013.

[5] Hirotaka Nakaya, Takayuki Matsuno, Tetsushi Kamegawa, Takao Hiraki, Takuya Inoue, Akira Yanou, Mamoru Minami, Akio Gofuku, "CT Phantom for Development of Robotic Interventional Radiology", IEEE/SICE International Symposium on System Integration, Chuo University, Tokyo, Japan, December 13-15, 2014.

[6] Kohei Sugiyama, Takayuki Matsuno, Tetsushi Kamegawa, Takao Hiraki, Hirotaka Nakaya, Akira Yanou, Mamoru Minami, "Reaction Force Analysis of Puncture Robot for CT-guided Interventional Radiology in Animal Experiment", IEEE/SICE International Symposium on System Integration (SII) December 11-13, 2015. Meijo University, Nagoya, Japan.

[7] John J. Craig, "Introduction to ROBOTICS - mechanics and control", Addison-Wesley, 1989.